ISSN 1392-5113 Nonlinear Analysis: Modelling and Control, 2018, Vol. 23, No. 2, 234–250
https://doi.org/10.15388/NA.2018.2.6

The robust finite-volume schemes for modeling nonclassical surface reactions

Raimondas Čiegis[a], **Pranas Katauskis**[b,1], **Vladas Skakauskas**[b]

[a]Vilnius Gediminas Technical University,
Saulėtekio ave. 11, LT-11203 Vilnius, Lithuania
raimondas.ciegis@vgtu.lt

[b]Faculty of Mathematics and Informatics, Vilnius University,
Naugarduko str. 24, LT-03225 Vilnius, Lithuania
pranas.katauskis@mif.vu.lt; vladas.skakauskas@mif.vu.lt

Received: May 24, 2017 / **Revised:** January 19, 2018 / **Published online:** February 12, 2018

Abstract. A coupled system of nonlinear parabolic PDEs arising in modeling of surface reactions with piecewise continuous kinetic data is studied. The nonclassic conjugation conditions are used at the surface of the discontinuity of the kinetic data. The finite-volume technique and the backward Euler method are used to approximate the given mathematical model. The monotonicity, conservativity, positivity of the approximations are investigated by applying these finite-volume schemes for simplified subproblems, which inherit main new nonstandard features of the full mathematical model. Some results of numerical experiments are discussed.

Keywords: system of nonlinear PDEs, finite-volume method, conservative approximation, heterogeneous reactions, surface diffusion, spillover.

1 Introduction

Coupled systems of PDEs with piecewise continuous (discontinuous) kinetic data typically arise in modeling of reactions proceeding over supported (composite) catalysts. Kinetic models of reactions proceeding over supported catalysts are of great complexity due to the spillover phenomenon, which is caused (i) by diffusion of molecules of reactants adsorbed on the surface of the inactive for reaction support towards the catalyst-support interface and their jump across the interface onto the active surface and (ii) by diffusion of adsorbate of reactants and intermediate reaction products towards the interface and their jump across the interface onto the support. This jumping can increase or reduce concentrations of molecules of all species involved in the surface reactions [5, 11].

Mathematical models describing the spillover phenomenon in some reactions taking into account the surface diffusion based on the diffusion model [7] and their numerical simulations are considered in [14, 15] and works mentioned there. The bibliography of

[1]Corresponding author.

the theoretical and experimental research of NO reduction by CO reaction can be found in [8, 9, 17]. To the best of our knowledge, the reaction between NO and CO on the supported catalysts has not been studied by a mean-field approach.

In the present paper, we present a phenomenological mathematical model for reactions between carbon monoxide and nitrogen oxide proceeding over the surface of supported catalysts. The model includes the adsorption and desorption of molecules of both reactants of prescribed concentrations at the surface and surface diffusion of adsorbed molecules. The model is based on the reaction mechanism proposed by Cho [2]. The surface diffusion of the adsorbed molecules is described by the jumping mechanism [7]. In what follows, we assume that the adsorption, desorption, surface diffusion, and reaction proceed at a constant temperature. We also construct a discrete scheme for numerical solving of this model.

Some results of the computer simulations varying initial concentrations of both reactants and their adsorption constants are presented.

The numerical scheme is based on the approximation of nonlinear differential equations by using the finite-volume method [10]. Three important properties of the model should be taken into account. First, the nonlinear reaction terms are describing processes for which a few specific properties of the solution are satisfied: the most important of them are the nonnegativity (or positivity) and a priori boundedness of the solutions. Thus discrete schemes should guarantee similar properties for the discrete solutions (see, e.g., [4, 10, 12]).

Second, the nonclassical (or nonideal) conjugation conditions are formulated at the catalyst-support interface. The mass conservation should be guaranteed for the discrete scheme. The solution is discontinuous at this boundary, thus special approximations should be used. Two general approaches exist to solve this problem: the discontinuous Galerkin method and application of special grids at the boundary. We use the second approach in this paper. In order to prove the existence and convergence of the discrete solution, the discrete operators approximating a diffusion part of the model should be positive definite.

Numerical algorithms for solving of some problems with nonclassical conjugation conditions are considered in [13, 16].

Third, the advection term enables a regularization of nonlinear diffusion-advection interaction [3]. In this paper, the upwind approximation is used for a numerical approximation of the advection term. An extensive review of results for numerical schemes for solving nonlinear complex reaction-diffusion-advection problems is given in [1, 6, 10, 12].

The discrete scheme of the differential model is too complicated to be mathematically justified. Therefore we split the model into some simplified benchmark submodels that mimic the most important properties of the full nonlinear model and investigate the monotonicity and positivity properties of the submodels.

The paper is organized as follows. In Section 2, we present the model. Section 3 consists of two subsections. Section 3.1 presents the finite-volume discretization and main implementation details. The implicit backward Euler scheme is used to approximate time derivatives. Two simplified parts of the full mathematical model are considered in Section 3.2. They mimic the most important properties of the full nonlinear differential

model. These simplified benchmark subproblems are used to test monotonicity of the discrete solution due to the main part of the nonlinear source terms and the stability and conservativity of approximation of nonstandard conjugate conditions. In Section 4, we discuss some results of computational experiments. A summary of main results in Section 5 concludes the paper.

2 The model

In this section, we construct a mean-field model for the $\mathrm{NO} + \mathrm{CO}$ reaction proceeding over the surface of a supported catalyst. Suppose that this surface lies on the plane $x_2 = 0$. Assume that concentrations $a_1(t, x_1, 0, x_3)$ and $a_2(t, x_1, 0, x_3)$ of reactants $\mathrm{A}_1 = \mathrm{NO}$ and $\mathrm{A}_2 = \mathrm{CO}$ are prescribed. Here t is time, and $(x_1, 0, x_3)$ is a position on the surface. Let $\mathrm{P}_1 = \mathrm{N_2O}$, $\mathrm{P}_2 = \mathrm{N}_2$, and $\mathrm{P}_3 = \mathrm{CO}_2$ be products of the reaction between A_1 and A_2. Assume that the surface of the catalyst $S = S_2 \cup S_1$, where $S_2 = \{(x_1, 0, x_3)\colon\ x_1 \in [0, x_*),\ x_3 \in [0, l]\}$ and $S_1 = \{(x_1, 0, x_3)\colon\ x_1 \in (x_*, l],\ x_3 \in [0, l]\}$, $x_* \in (0, l)$, are strips consisting of the active and inactive sites, respectively. Let $s_2(x)$, $x = (x_1, 0, x_3) \in S_2$, and $s_1(x)$, $x = (x_1, 0, x_3) \in S_1$, be the surface densities of the active and inactive sites in the surface reaction.

According to [2, 17], the surface $\mathrm{NO} + \mathrm{CO}$ reaction is based on the NO reduction reaction by CO, $4\mathrm{NO} + 3\mathrm{CO} \to \mathrm{N_2O} + 3\mathrm{CO}_2 + \mathrm{N}_2$, which occur via steps

$$\mathrm{NO} + \mathrm{S} \underset{k_{-1i}}{\overset{k_{1i}}{\rightleftarrows}} \mathrm{NOS},$$

$$\mathrm{CO} + \mathrm{S} \underset{k_{-2i}}{\overset{k_{2i}}{\rightleftarrows}} \mathrm{COS},$$

$$\mathrm{NOS} + \mathrm{S} \overset{k_{32}}{\to} \mathrm{NS} + \mathrm{OS},$$

$$\mathrm{NOS} + \mathrm{NS} \overset{k_{42}}{\to} \mathrm{N_2O} + 2\mathrm{S},$$

$$2\mathrm{NS} \overset{k_{52}}{\to} \mathrm{N}_2 + 2\mathrm{S},$$

$$\mathrm{COS} + \mathrm{OS} \overset{k_{62}}{\to} \mathrm{CO}_2 + 2\mathrm{S}.$$

Here S is the adjacent vacant adsorption site, k_{ji} and k_{-ji} are the adsorption and desorption rate constants ($i = 1$ for inactive and $i = 2$ for active site) of reactants A_1 ($j = 1$) and A_2 ($j = 2$), k_{j2} with $j = 3, 4, 5, 6$ are the reaction rate constants.

Let $u_{j2} = s_2\theta_{j2}$ and $u_{j1} = s_1\theta_{j1}$ ($\theta_{j1}, \theta_{j2} \in (0, 1)$, $j = 1, \dots, 4$) be densities of the active and inactive in the surface reaction sites occupied by adsorbed particles of reactants A_1 ($j = 1$) and A_2 ($j = 2$) and molecules of species NS ($j = 3$), OS ($j = 4$). It is evident that function $s_i(1 - \sum_{j=1}^{4} \theta_{ji}) = s_i - \sum_{j=1}^{4} u_{ji}$ is the density of free active ($i = 2$) and inactive ($i = 1$) adsorption sites.

Suppose that κ_{ji} is the surface diffusivity for particles of species NOS, COS, NS, and OS with $j = 1, \dots, 4$, respectively, on the surface S_i, $i = 1, 2$. In what follows, for the sake of simplicity, we assume that densities s_1 and s_2 do not depend on variable x_3, and

the concentrations a_1 and a_2 are constants. This allows us to reduce the two-dimensional problem into the one-dimensional system. For simplification in what follows, we denote variable x_1 by x. Assume that $\lambda_{1,j2}$, $j = 1, \dots, 4$, is the constant of the jumping rate via the catalyst-support interface x_* of particles of species NOS, COS, NS, and OS from the active position $x_* - 0$ into the nearest-neighbour vacant inactive site $x_* + 0$. Let $\lambda_{2,j1}$ be the constants of the jump rates via the catalyst-support interface of the particles of the same species from the inactive position $x_* + 0$ into the nearest-neighbour vacant active site $x_* - 0$. Using the mass action law and surface diffusion mechanism [7],

$$q_{ji} = -\kappa_{ji}\left\{\left(s_i - \sum_{m=1}^{4} u_{mi}\right)\nabla u_{ji} - u_{ji}\nabla\left(s_i - \sum_{m=1}^{4} u_{mi}\right)\right\},$$

where $i = 1, 2$, $j = 1, \dots, 4$, we derive the following system for densities u_{ji}:

$$\begin{aligned}
\partial_t u_{11} &= k_{11}a_1\left(s_1 - \sum_m u_{m1}\right) - k_{-11}u_{11} \\
&\quad + \kappa_{11}\left(\left(s_1 - \sum_{m\neq 1} u_{m1}\right)\frac{\partial^2 u_{11}}{\partial x^2} - u_{11}\frac{\partial^2(s_1 - \sum_{m\neq 1} u_{m1})}{\partial x^2}\right), \\
\partial_t u_{21} &= k_{21}a_2\left(s_1 - \sum_m u_{m1}\right) - k_{-21}u_{21} \\
&\quad + \kappa_{21}\left(\left(s_1 - \sum_{m\neq 2} u_{m1}\right)\frac{\partial^2 u_{21}}{\partial x^2} - u_{21}\frac{\partial^2(s_1 - \sum_{m\neq 2} u_{m1})}{\partial x^2}\right), \\
\partial_t u_{31} &= \kappa_{31}\left(\left(s_1 - \sum_{m\neq 3} u_{m1}\right)\frac{\partial^2 u_{31}}{\partial x^2} - u_{31}\frac{\partial^2(s_1 - \sum_{m\neq 3} u_{m1})}{\partial x^2}\right), \\
\partial_t u_{41} &= \kappa_{41}\left(\left(s_1 - \sum_{m\neq 4} u_{m1}\right)\frac{\partial^2 u_{41}}{\partial x^2} - u_{41}\frac{\partial^2(s_1 - \sum_{m\neq 4} u_{m1})}{\partial x^2}\right)
\end{aligned} \tag{1}$$

with $x \in (x_*, l)$,

$$\begin{aligned}
\partial_t u_{12} &= (k_{12}a_1 - k_{32}u_{12})\left(s_2 - \sum_m u_{m2}\right) - k_{-12}u_{12} - k_{42}u_{12}u_{32} \\
&\quad + \kappa_{12}\left(\left(s_2 - \sum_{m\neq 1} u_{m2}\right)\frac{\partial^2 u_{12}}{\partial x^2} - u_{12}\frac{\partial^2(s_2 - \sum_{m\neq 1} u_{m2})}{\partial x^2}\right), \\
\partial_t u_{22} &= k_{22}a_2\left(s_2 - \sum_m u_{m2}\right) - k_{-22}u_{22} - k_{62}u_{22}u_{42} \\
&\quad + \kappa_{22}\left(\left(s_2 - \sum_{m\neq 2} u_{m2}\right)\frac{\partial^2 u_{22}}{\partial x^2} - u_{22}\frac{\partial^2(s_2 - \sum_{m\neq 2} u_{m2})}{\partial x^2}\right),
\end{aligned} \tag{2a}$$

$$
\begin{aligned}
\partial_t u_{32} &= k_{32}u_{12}\biggl(s_2 - \sum_m u_{m2}\biggr) - k_{42}u_{12}u_{32} - 2k_{52}u_{32}^2 \\
&\quad + \kappa_{32}\biggl(\biggl(s_2 - \sum_{m\neq 3} u_{m2}\biggr)\frac{\partial^2 u_{32}}{\partial x^2} - u_{32}\frac{\partial^2(s_2 - \sum_{m\neq 3} u_{m2})}{\partial x^2}\biggr), \\
\partial_t u_{42} &= k_{32}u_{12}\biggl(s_2 - \sum_m u_{m2}\biggr) - k_{62}u_{22}u_{42} \\
&\quad + \kappa_{42}\biggl(\biggl(s_2 - \sum_{m\neq 4} u_{m2}\biggr)\frac{\partial^2 u_{42}}{\partial x^2} - u_{42}\frac{\partial^2(s_2 - \sum_{m\neq 4} u_{m2})}{\partial x^2}\biggr)
\end{aligned}
\tag{2b}
$$

with $x \in (0, x_*)$. Here and in what follows, ∂_t signifies the partial derivative with respect to time and $\sum_m u_{mi} = \sum_{m=1}^4 u_{mi}$. We add to this system the initial,

$$
u_{ji}(0, x) = 0, \quad j = 1, \ldots, 4,\ i = 1, 2, \tag{3}
$$

and boundary conditions at points $x = 0$, $x = l$, $x = x_*$,

$$
\left.\frac{\partial u_{j2}}{\partial x}\right|_{x=0} = \left.\frac{\partial u_{j1}}{\partial x}\right|_{x=l} = 0, \quad j = 1, \ldots, 4, \tag{4}
$$

$$
\begin{aligned}
&\kappa_{j1}\biggl(\biggl(s_1 - \sum_{m\neq j} u_{m1}\biggr)\frac{\partial u_{j1}}{\partial x} - u_{j1}\frac{\partial(s_1 - \sum_{m\neq j} u_{m1})}{\partial x}\biggr)\biggr|_{x_*+0} \\
&\quad = \kappa_{j2}\biggl(\biggl(s_2 - \sum_{m\neq j} u_{m2}\biggr)\frac{\partial u_{j2}}{\partial x} - u_{j2}\frac{\partial(s_2 - \sum_{m\neq j} u_{m2})}{\partial x}\biggr)\biggr|_{x_*-0} \\
&\quad = \lambda_{2,j1}u_{j1}|_{x_*+0}\biggl(s_2 - \sum_m u_{m2}\biggr)\biggr|_{x_*-0} \\
&\qquad - \lambda_{1,j2}u_{j2}|_{x_*-0}\biggl(s_1 - \sum_m u_{m1}\biggr)\biggr|_{x_*+0}, \quad j = 1, \ldots, 4.
\end{aligned}
\tag{5}
$$

System (1)–(5) determines densities u_{ji} for all $x \in S$ and $t > 0$. We determine the surface S_2 specific conversion rate of molecules of both reactants into the product ones (turn-over rate or turn-over frequency) by the formulas

$$
z_1 = \int_0^{x_*} k_{42}u_{12}u_{32}\,\mathrm{d}x \Big/ \int_0^{x_*} s_2\,\mathrm{d}x, \qquad z_2 = \int_0^{x_*} k_{52}u_{32}^2\,\mathrm{d}x \Big/ \int_0^{x_*} s_2\,\mathrm{d}x,
$$

and

$$
z_3 = \int_0^{x_*} k_{62}u_{22}u_{42}\,\mathrm{d}x \Big/ \int_0^{x_*} s_2\,\mathrm{d}x
$$

for products P_1, P_2, and P_3, respectively.

Using the dimensionless variables

$$\begin{aligned}
&\bar{t} = \frac{t}{T}, \quad \bar{x} = \frac{x}{l}, \quad \bar{a}_i = \frac{a_i}{a_*}, \quad s_* = la_*, \quad \bar{k}_{ij} = k_{ij}Ta_*, \quad \bar{k}_{-ij} = k_{-ij}T, \\
&\bar{k}_{32} = k_{32}T, \quad \bar{k}_{42} = Ts_*k_{42}, \quad \bar{k}_{52} = Ts_*k_{52}, \quad \bar{k}_{62} = Ts_*k_{62}, \\
&\bar{s}_i = \frac{s_i}{s_*}, \quad \bar{\lambda}_{n,mi} = a_*T\lambda_{n,mi}, \quad \bar{\kappa}_{mi} = \frac{\kappa_{mi}a_*T}{l}, \quad \bar{u}_{mi} = \frac{u_{mi}}{s_*} = \bar{s}_i\theta_{mi},
\end{aligned} \tag{6}$$

where $i, j, n = 1, 2$, $m = 1, \ldots, 4$, and $T = 1$ s, $l = 10^{-1}$ cm, $a_* = 10^{-11}$ mol cm^{-3}, $s_* = 10^{-12}$ mol cm^{-2} are the characteristic dimensional units, we rewrite Eqs. (1)–(5) in the same form, but in dimensionless variables. For the sake of simplicity, we omit the overbar on the quantities and consider Eqs. (1)–(5) as dimensionless.

3 Discrete approximation

This section consists of two subsections. Section 3.1 presents the finite-volume discretization of the given mathematical model and main implementation details. Two simplified parts of the full mathematical model are considered in Section 3.2. They mimic the most important properties of the full nonlinear differential model. These simplified benchmark subproblems are used to test monotonicity of the solution due to the main part of the nonlinear source terms and the stability of approximation of nonclassical conjugate conditions. It should be noted that the theoretical analysis of Section 3.2 is strictly valid only for the simplified models.

3.1 Finite-volume approximation

We rewrite Eqs. (1), (2) in a short form

$$\begin{aligned}
&\partial_t u_{m1} = f_{m1}(u_1) + L_{m1}(u_1), \quad x^* < x < 1, \\
&\partial_t u_{m2} = f_{m2}(u_2) + L_{m2}(u_2), \quad 0 < x < x^*,
\end{aligned} \tag{7}$$

where $m = 1, \ldots, 4$, $u_k = (u_{1k}, \ldots, u_{4k})$, $k = 1, 2$, f_{mk} define nonlinear reaction terms, and L_{mk} define diffusion operators

$$L_{mk}(u_k) = \frac{\partial}{\partial x} J_{mk}(u_k),$$

and the flux is rewritten in the following form:

$$J_{mk}(u_k) = \kappa_{mk}\left(\left(s_k - \sum_{j \neq m} u_{jk}\right)\frac{\partial u_{mk}}{\partial x} - u_{mk}\frac{\partial}{\partial x}\left(s_k - \sum_{j \neq m} u_{jk}\right)\right).$$

The domain $\bar{D} = \bar{D}_2 \cup \bar{D}_1 = [0, x^*] \cup [x^*, 1]$ is covered by the discrete uniform grid $\bar{D}_h = \bar{D}_{2h} \cup \bar{D}_{1h}$:

$$\begin{aligned}
&\bar{D}_{1h} = \{x_j\colon\ x_j = x^* + jh_1,\ j = 0, \ldots, J_1\}, \quad x_{J_1} = 1, \\
&\bar{D}_{2h} = \{x_j\colon\ x_j = jh_2,\ j = 0, \ldots, J_2\}, \quad x_{J_2} = x^*,
\end{aligned}$$

and $\bar{D}_{kh} = D_{kh} \cup \partial D_{kh}$. Let ω_τ be a uniform time grid

$$\omega_\tau = \{t^n\colon\ t^n = n\tau,\ n = 0, \dots, N,\ N\tau = T\},$$

where τ is the time step. A more general nonuniform/adaptive grid can be used directly, and the uniform grid is applied only to simplify the notation.

We consider numerical approximations $U^n_{mk,j}$ to the exact solution values $u^n_{mk,j} = u_{mk}(x_j, t^n)$ at the grid points $(x_j, t^n) \in \bar{D}_{kh} \times \omega_\tau$.

For functions defined on the grid, we introduce the forward and backward difference quotients with respect to x

$$\delta_x U^n_{k,j} = \frac{U^n_{k,j+1} - U^n_{k,j}}{h_k}, \qquad \delta_{\bar{x}} U^n_{k,j} = \frac{U^n_{k,j} - U^n_{k,j-1}}{h_k}$$

and similarly the backward difference quotient with respect to time t

$$\delta_{\bar{t}} U^n_j = \frac{U^n_j - U^{n-1}_j}{\tau}.$$

We apply the finite-volume method and approximate the system of differential equations (7) by the nonlinear discrete scheme

$$\delta_{\bar{t}} U^n_{mk,j} = f_{mk}\big(U^n_{k,j}\big) + L_{h,mk,j}\big(U^n_k\big), \quad x_j \in D_{hk}, \tag{8}$$

where $n > 0$, $m = 1, \dots, 4$, $k = 1, 2$, and the discrete operator L_h is defined as

$$L_{h,mk,j}(U_k) = \delta_x J_{h,mk,j-1/2}(U_k).$$

Here we use the following definitions:

$$\delta_x J_{h,mk,j-1/2} = \frac{J_{h,mk,j+1/2} - J_{h,mk,j-1/2}}{h_k},$$

$$J_{h,mk,j-1/2}(U_k) = \kappa_{mk}\Bigg\{\Bigg(s_k - \sum_{i\neq m} \frac{1}{2}(U_{ik,j} + U_{ik,j-1})\Bigg)\delta_{\bar{x}} U_{mk,j} - U^*_{mk,j}\delta_{\bar{x}}\Bigg(s_k - \sum_{i\neq m} U_{ik,j}\Bigg)\Bigg\},$$

$$U^*_{mk,j} = \begin{cases} U_{mk,j-1} & \text{if } \delta_{\bar{x}}(s_k - \sum_{i\neq m} U_{ik,j}) \geqslant 0, \\ U_{mk,j} & \text{if } \delta_{\bar{x}}(s_k - \sum_{i\neq m} U_{ik,j}) < 0. \end{cases}$$

We note that the upwind approximation is used in the definition of the discrete flux, i.e., the second part of the flux is treated as a nonlinear advection term. This approach was used in [3] for a numerical simulation of bacterial self-organization processes.

Since s_k are constants, $k = 1, 2$, the boundary conditions (4) are changed to equivalent conditions

$$J_{m2}|_{x=0} = 0, \quad J_{m1}|_{x=1} = 0, \quad m = 1, \dots, 4,$$

and they are directly included into the finite-volume balance equations:

$$J_{h,m2,1/2}\big(U_2^n\big) - \frac{h_2}{2}\big(\delta_{\bar{t}}U^n_{m2,0} - f_{m2}\big(U^n_{2,0}\big)\big) = 0, \tag{9}$$

$$J_{h,m1,J_1-1/2}\big(U_1^n\big) + \frac{h_1}{2}\big(\delta_{\bar{t}}U^n_{m1,J_1} - f_{m1}\big(U^n_{1,J_1}\big)\big) = 0. \tag{10}$$

At $x = x^*$, the discrete conjugation conditions are formulated:

$$\begin{aligned} &J_{h,m1,1/2}\big(U_1^n\big) - \frac{h_1}{2}\big(\delta_{\bar{t}}U^n_{m1,0} - f_{m1}\big(U^n_{1,0}\big)\big) \\ &\quad = J_{h,m2,J_2-1/2}\big(U_2^n\big) + \frac{h_2}{2}\big(\delta_{\bar{t}}U^n_{m2,J_2} - f_{m2}\big(U^n_{2,J_2}\big)\big), \end{aligned} \tag{11}$$

$$\begin{aligned} &J_{h,m2,J_2-1/2}\big(U_2^n\big) + \frac{h_2}{2}\big(\delta_{\bar{t}}U^n_{m2,J_2} - f_{m2}\big(U^n_{2,J_2}\big)\big) \\ &\quad = \lambda_{2,m1}U^n_{m1,0}\bigg(s_2 - \sum_l U^n_{l2,J_2}\bigg) - \lambda_{1,m2}U^n_{m2,J_2}\bigg(s_1 - \sum_l U^n_{l1,0}\bigg). \end{aligned} \tag{12}$$

Iterative algorithm. At each time step, the solution of discrete nonlinear system (8)–(12) is computed by using a Jacobi-type iterative algorithm. For all (m,k,j), source terms f_{mk} are linearized with respect to $U^n_{mk,j}$, e.g., to compute new iteration $U^{n,p}_{42,j}$, we use

$$f_{42}(U_{2,j}) = k_{32}U^{n,p-1}_{12,j}\bigg(s_2 - \sum_{m\neq 4} U^{n,p-1}_{m2,j} - U^{n,p}_{42,j}\bigg) - k_{62}U^{n,p-1}_{22,j}U^{n,p}_{42,j}.$$

Operators $L_{h,mk,j}$ are linearized with respect to $U^n_{mk,j}$, $U^n_{mk,j\pm1}$:

$$\begin{aligned} J_{h,mk,j-1/2}(U_k) = \kappa_{mk}\Bigg\{&\bigg(s_k - \sum_{i\neq m}\frac{1}{2}\big(U^{n,p-1}_{ik,j} + U^{n,p-1}_{ik,j-1}\big)\bigg)\delta_{\bar{x}}U^{n,p}_{mk,j} \\ &- U^{*,p}_{mk,j}\delta_{\bar{x}}\bigg(s_k - \sum_{i\neq m}U^{n,p-1}_{ik,j}\bigg)\Bigg\}. \end{aligned}$$

A matrix of the obtained system of linear equations is tridiagonal, and it can be solved efficiently by using the factorization method.

3.2 Theoretical analysis of simplified subproblems

In this section, we consider two simplified models, which inherit the most interesting properties of the full mathematical model and apply the finite-volume scheme developed in the previous section. The selected subproblems are used to test monotonicity of the discrete solution due to the main part of nonlinear source terms and the stability of the finite-volume approximation of nonclassical conjugate conditions.

3.2.1 Monotonicity of the discrete scheme for reactions

In this section, we investigate the monotonicity of the approximation of reactions for the following benchmark problem:

$$\frac{du_j}{dt} = k_j\biggl(C - \sum_m u_m(t)\biggr), \quad j = 1, \dots, 4,$$
$$u_j(0) = 0, \quad k_j > 0,\ C > 0.$$

In this system of ODEs, we have omitted sink terms $(-k_{-j}u_j)$ since they only reduce the maximum value of the solution. A simple analysis gives that

$$u_j(t) \geqslant 0, \quad \sum_m u_m(t) \leqslant C.$$

We approximate the given problem by the backward Euler scheme

$$\delta_{\bar{t}} U_j^n = k_j\biggl(C - \sum_m U_m^n\biggr), \quad U_j^0 = 0,\ j = 1, \dots, 4. \tag{13}$$

Theorem 1. *The following positivity and boundedness* (*PB*) *estimates*

$$U_j^n \geqslant 0, \quad j = 1, \dots, 4, \quad C - \sum_m U_m^n \geqslant 0, \quad n \geqslant 0,$$

are valid for the solution of (13).

Proof. Adding all equations (13) and taking into account that C is constant, we get the equation

$$\delta_{\bar{t}}\biggl(C - \sum_m U_m^n\biggr) = -\sum_m k_m\biggl(C - \sum_m U_m^n\biggr).$$

Solving it and taking into account initial conditions gives the second required estimate

$$\begin{aligned} C - \sum_m U_m^n &= \frac{1}{1 + \tau\sum_m k_m}\biggl(C - \sum_m U_m^{n-1}\biggr) \\ &= \cdots = \biggl(\frac{1}{1 + \tau\sum_m k_m}\biggr)^n C \geqslant 0. \end{aligned} \tag{14}$$

It follows from Eqs. (13) that the solution can be written as

$$U_j^n = k_j \Phi^n, \quad j = 1, \dots, 4.$$

Substituting this expression into (14), we get Φ^n in the explicit form:

$$\Phi^n = C\biggl[1 - \biggl(\frac{1}{1 + \tau\sum_m k_m}\biggr)^n\biggr] \Big/ \sum_m k_m \geqslant 0.$$

Thus the solution $U_m^n \geqslant 0$. □

3.2.2 Stability of the finite-volume scheme for approximation of nonstandard conjugation conditions

In this section, our main aim is to investigate the stability of the finite-volume scheme when nonstandard conjugation conditions are used. Thus we restrict to a simplified subproblem of the general mathematical model and investigate in detail the influence of new conjugation conditions. As a subproblem, we consider the following linear initial-boundary value parabolic problem:

$$\begin{aligned}
&\partial_t u = \frac{\partial^2 u}{\partial x^2} + f(x,t), \quad 0 < x < 1,\ t > 0,\\
&\left.\frac{\partial u}{\partial x}\right|_{x^*-0} = \left.\frac{\partial u}{\partial x}\right|_{x^*+0} = \alpha\big(u(x^*+0,t) - u(x^*-0,t)\big),\\
&u(0,t) = 0, \quad u(1,t) = 0\\
&u(x,0) = u_0(x), \quad 0 \leqslant x \leqslant 1.
\end{aligned}$$

Next, we approximate it by using the finite-volume discretization similar to (8) and get the following discrete scheme:

$$\begin{aligned}
&\delta_{\bar{t}} U_j^n + A_h U^n = F_j^n, \quad j = 1,\dots,J-1,\\
&U_0^n = 0, \quad U_J^n = 0,\\
&U_j^0 = u_0(x_j), \quad j = 0,\dots,J,
\end{aligned} \tag{15}$$

where the discrete operator A_h is defined as

$$A_h U = \begin{cases}
-\delta_x \delta_{\bar{x}} U_j, & 0 < j \neq K, K+1 < J,\\
\frac{2}{h}(\delta_{\bar{x}} U_K - \alpha(U_{K+1} - U_K)), & j = K,\\
-\frac{2}{h}(\delta_x U_{K+1} - \alpha(U_{K+1} - U_K)), & j = K+1,
\end{cases}$$

where we use notation $K = J_2$, and $0 < K < J$.

We define the scalar product

$$(U,V) = (U,V)_1 + (U,V)_2,$$

where

$$\begin{aligned}
(U,V)_1 &= \sum_{j=1}^{K-1} hU_jV_j + \frac{h}{2}U_KV_K,\\
(U,V)_2 &= \sum_{j=K+2}^{J-1} hU_jV_j + \frac{h}{2}U_{K+1}V_{K+1}.
\end{aligned}$$

Also we define the following discrete inner products:

$$(U,V]_1 = \sum_{j=1}^{K} hU_jV_j, \qquad (U,V]_2 = \sum_{j=K+2}^{J} hU_jV_j.$$

Lemma 1. *The discrete operator A_h is symmetric and positive definite*

$$A_h = A_h^* \geqslant \lambda_0 I, \quad \lambda_0 > 0.$$

Proof. Multiplying $A_h U$ by V, using the summation by parts formula and the definition of $A_h U$ for $j = K, K+1$, we get the equality

$$(A_h U, V) = (\partial_{\bar{x}} U, \partial_{\bar{x}} V]_1 + (\partial_{\bar{x}} U, \partial_{\bar{x}} V]_2 + \alpha(U_{K+1} - U_K)(V_{K+1} - V_K),$$

which proves that operator A_h is symmetric. Taking $V = U$, we get that

$$(A_h U, U) = (\partial_{\bar{x}} U, \partial_{\bar{x}} U]_1 + (\partial_{\bar{x}} U, \partial_{\bar{x}} U]_2 + \alpha(U_{K+1} - U_K)^2,$$

thus $A_h \geqslant 0$.

Next, using a discrete Friedrich–Poincaré-type inequality, we prove that [12]

$$(\partial_{\bar{x}} U, \partial_{\bar{x}} U]_j \geqslant \lambda_{0j} (U, U)_j, \quad \lambda_{0j} > 0,\ j = 1, 2.$$

Combining both estimates, we get that A_h is positive definite:

$$(A_h U, U) \geqslant (\partial_{\bar{x}} U, \partial_{\bar{x}} U]_1 + (\partial_{\bar{x}} U, \partial_{\bar{x}} U]_2 \geqslant \min(\lambda_{01}, \lambda_{02})(U, U). \qquad \square$$

Next, using standard stability analysis techniques, we prove apriori stability estimates.

Theorem 2. *The discrete scheme* (15) *is stable and the following stability estimates are valid*:

$$\|U^n\| \leqslant \|U^{n-1}\| + \tau \|F^n\|, \tag{16}$$

$$\|U^n\|^2 \leqslant \|U^{n-1}\|^2 + \frac{\tau}{2} \|F^n\|^2_{A_h^{-1}}, \tag{17}$$

where the L_2 norm is defined as $\|U\|^2 = (U, U)$ and $\|U\|^2_{A_h^{-1}} = (A_h^{-1} U, U)$.

Proof. Multiplying (15) by U^n gives

$$\begin{aligned} \big(U^n, U^n\big) + \tau \big(A_h U^n, U^n\big) &= \big(U^n, U^{n-1}\big) + \tau \big(F^n, U^n\big) \\ &\leqslant \|U^n\| \, \|U^{n-1}\| + \tau \|F^n\| \, \|U^n\|, \end{aligned}$$

from which and Lemma 1 the first stability estimate (16) follows.

In order to prove the second stability estimate (17), we again multiply Eq. (15) by U^n and evaluate the right-hand side as

$$\begin{aligned} \big(U^n, U^{n-1}\big) + \tau \big(F^n, U^n\big) \leqslant{}& \frac{1}{2} \|U^n\|^2 + \frac{1}{2} \|U^{n-1}\|^2 + \frac{\tau}{4} \|F^n\|^2_{A_h^{-1}} \\ &+ \tau \big(A_h U^n, U^n\big). \end{aligned}$$

Note that, in order to prove the stability estimate (16), it is sufficient to assume that $A_h \geqslant 0$. $\square$

Similarly, we can analyze more general nonstandard conjugation conditions defined as

$$A_hU=\begin{cases}-\partial_x\partial_{\bar{x}}U_j, & 0<j\neq K,\ K+1<J,\\ \frac{2}{h}(\partial_{\bar{x}}U_K-(\alpha_2U_{K+1}-\alpha_1U_K)), & j=K,\\ -\frac{2}{h}(\partial_xU_{K+1}-(\alpha_2U_{K+1}-\alpha_1U_K)), & j=K+1,\end{cases}$$

where $\alpha_1,\alpha_2>0$. Multiplying (15) by α_1V_j for $j=1,\dots,K-1$ and α_2V_j for $j=K+2,\dots,J-1$ gives a weak formulation of the problem

$$\begin{aligned}&\alpha_1\big(U^n,V\big)_1+\alpha_2\big(U^n,V\big)_2+\tau\big[\alpha_1\big(\partial_{\bar{x}}U^n,\partial_{\bar{x}}V\big]_1+\alpha_2\big(\partial_{\bar{x}}U^n,\partial_{\bar{x}}V\big]_2\\ &\quad+\big(\alpha_2U^n_{K+1}-\alpha_1U^n_K\big)(\alpha_2V_{K+1}-\alpha_1V_K)\big]\\ &=\alpha_1\big(U^{n-1},V\big)_1+\alpha_2\big(U^{n-1},V\big)_2+\tau\big[\alpha_1\big(F^n,V\big)_1+\alpha_2\big(F^n,V\big)_2\big],\end{aligned}$$

from which similar apriori stability estimates are derived in the L_2 norm induced by the scalar product

$$(U,V)=\alpha_1(U,V)_1+\alpha_2(U,V)_2.$$

4 Some results of computational experiments

For calculations, we used the following values of dimensionless parameters excluding those given in captions:

$$\begin{aligned}k_{ij}&=1.5\cdot10^{-2},\quad k_{-ij}=1.5\cdot10^{-3},\quad i,j=1,2;\\ \lambda_{n,ij}&=0.01,\quad n,j=1,2,\ i=1,\dots,4;\qquad a_1=a_2=1;\\ \kappa_{ij}&=0.01,\quad i=1,\dots,4,\ j=1,2;\qquad x_*=0.5,\\ k_{i2}&=0.01,\quad i=3,\dots,6;\qquad s_1=s_2=1.\end{aligned}$$

These values are calculated from the dimensional values (6). Some numerical results are illustrated in Figs. 1–5.

Figure 1 illustrates the dependence of the turn-over rates $z_1(t)$ and $z_2(t)$ on the variation of the concentrations of reactants NO and CO. Both functions are nonmonotonic in time: rapidly grow, attain the maximal values, and then decrease as time grows. For large t and $a_1=1$, conversion rates $z_1(t)$ and $z_2(t)$ are decreasing functions of the CO concentration a_2, but for small t, they are nonmonotonic functions of a_2.

For large time and $a_2=1$, function z_1 grows, reaches maximum values, and then decreases as a_1 increases. The $\max_t z_1(t)$ also increases as a_1 grows, possesses a maximum value at some $a_1\approx3$, and then decreases. Figure 1(b) shows that the increase of NO concentration a_1 decreases $\max_t z_2(t)$. Moreover, from Fig. 1(b) we observe the more rapid decrease of z_2 over time as the concentration of NO a_1 grows.

Plots in Fig. 2 demonstrate the influence of the adsorption rate constants k_{11} and k_{21} of the reactants NO and CO on the turn-over rates $z_2(t)$ and $z_3(t)$ in the case where both reactants adsorb only on the inactive in reaction domain S_{21} with $k_{12}=k_{22}=0$.

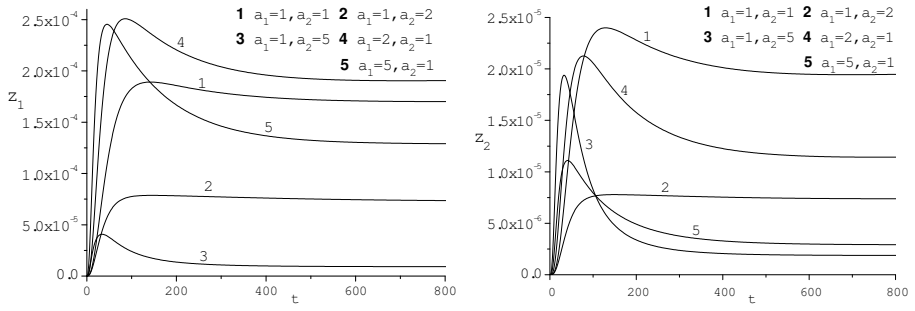

Figure 1. Dependence of time profiles of the turn-over rates $z_1(t)$ and $z_2(t)$ on the variation of the concentrations of reactants.

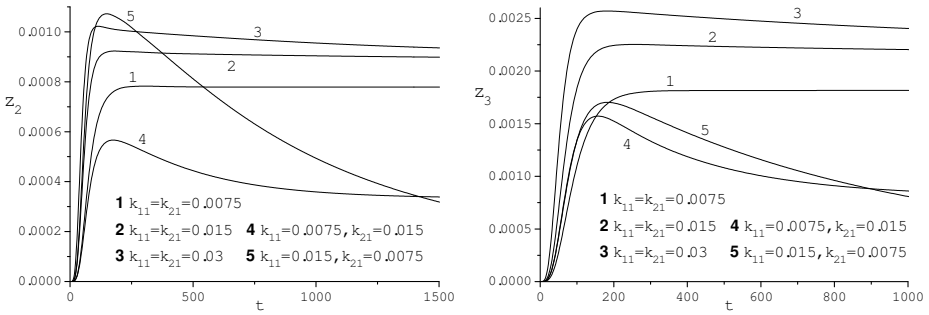

Figure 2. Effect of the variation of the adsorption rate constants k_{11} and k_{21} on the turn-over rates $z_2(t)$ and $z_3(t)$ calculated for the reactant concentrations $a_1 = a_2 = 1$ in case $k_{12} = k_{22} = 0$.

The surface reaction proceeds only due to the spillover effect. Calculations shows that the effect of parameters k_{11} and k_{21} on the conversion rates $z_1(t)$ (results not shown) and $z_2(t)$ is similar.

From Figs. 2(a) and 2(b) we observe that both turn-over rates $z_2(t)$ and $z_3(t)$ are nonmonotonic time functions. Values of $z_2(t)$ and $z_3(t)$ increase as the same adsorption rate constant of both reactants for the inactive domain $k_{11} = k_{21}$ grows. The effect of the adsorption rate constant of NO and CO on the turn-over rates is different. Values of functions $z_2(t)$ and $z_3(t)$ decrease as the adsorption rate of reactant CO grows (curves 1 and 4). From Fig. 2(a) we see that the increase of the adsorption rate of NO substantially increases $z_2(t)$ for small t, but for large t, function $z_2(t)$ behaves vice versa (curves 1 and 5). Figure 2(b) shows that the growth of k_{11} decreases $z_3(t)$. Moreover, we observe the more rapid decrease of $z_2(t)$ and $z_3(t)$ over time as either the adsorption rate constant k_{11} or k_{21} grows in comparison with the case when $k_{11} = k_{21}$ increases.

Figures 3 and 4 demonstrate the spillover effect on the concentrations $u_{ji}(t_k, x)$, $j, i = 1, 2$, for $a_1 = 2$, $a_2 = 1$, and fixed values of time $t_1 = 20$, $t_2 = 100$, $t_3 = 500$

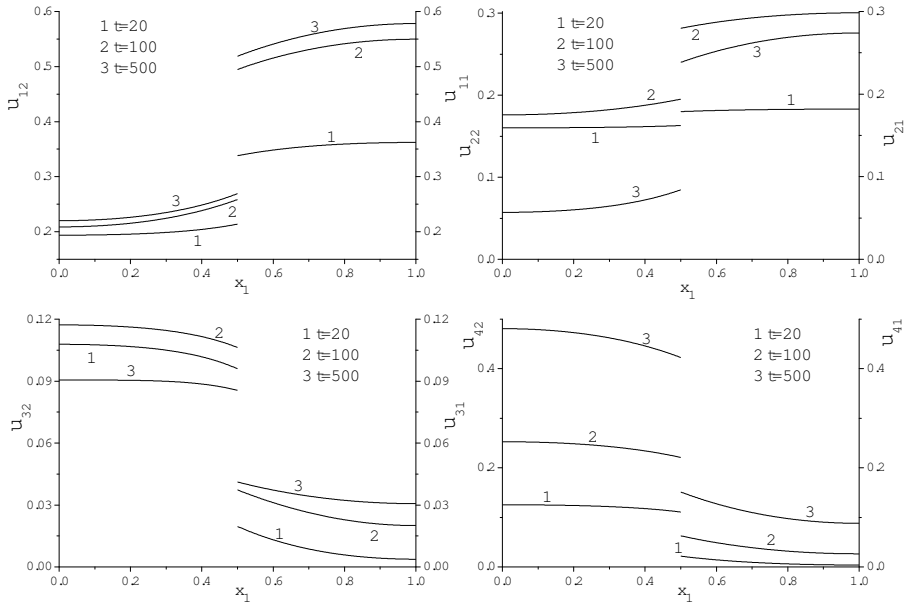

Figure 3. Influence of the spillover on the concentrations u_{ji}, $j, i = 1, 2$, for $a_1 = 2$, $a_2 = 1$ when both reactants adsorb on the inactive and active surfaces.

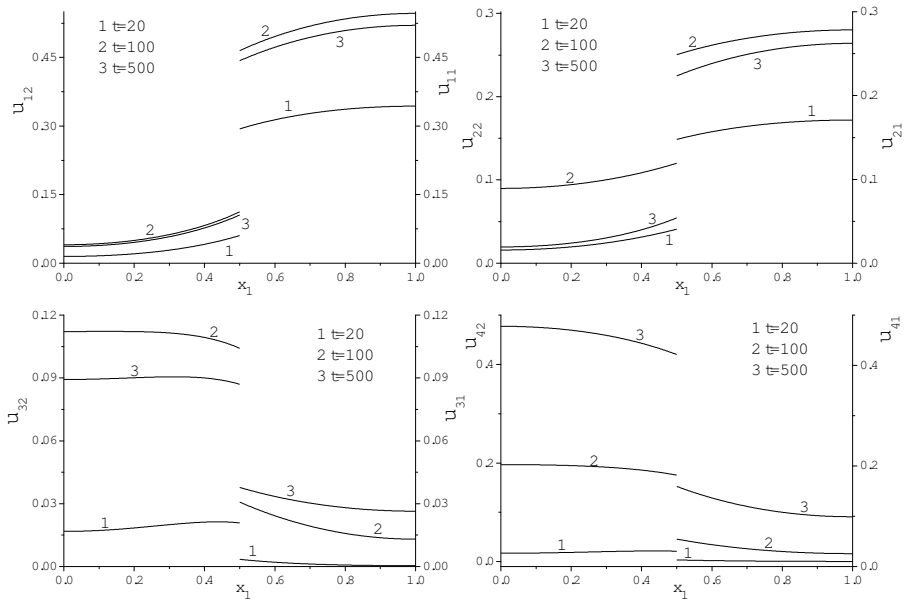

Figure 4. Effect of the spillover on the concentrations u_{ji}, $j, i = 1, 2$, for $a_1 = 2$, $a_2 = 1$ when both reactants adsorb only on the inactive surfaces.

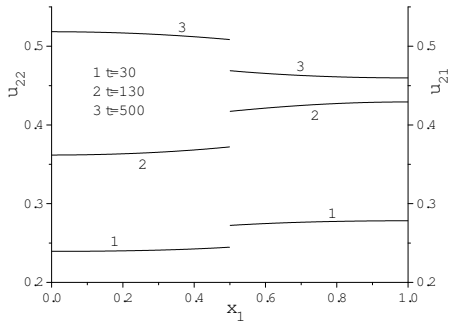

Figure 5. Dependence of the concentrations u_{21} and u_{22} on the spillover effect when $a_1 = a_2 = 1$ and both reactants adsorb on the inactive and active surfaces.

in two cases of reactants adsorption: (i) both reactants adsorb on the inactive and active surfaces (Fig. 3), (ii) they adsorb only on the inactive surface (Fig. 4). In case (ii), the reaction $\mathrm{CO} + \mathrm{NO}$ occurs only due to the spillover phenomenon. Graphs of functions $u_{11}(t_k, x)$, $u_{21}(t_k, x)$ defined on the inactive surface $(x_*, 1]$ and of $u_{3,2}(t_k, x)$, $u_{4,2}(t_k, x)$ defined on the active surface $[0, x_*)$ are concave. Graphs of $u_{1,2}(t_k, x)$, $u_{2,2}(t_k, x)$ defined on $[0, x_*)$ and $u_{3,1}(t_k, x)$, $u_{4,1}(t_k, x)$ defined on $(x_*, 1]$ are convex. All functions $u_{ji}(t_k, x)$ are discontinuous at the catalyst-support interface $x_* = 0.5$.

Plots in Fig. 5 illustrate the spillover influence on the behavior of concentrations $u_{21}(t_k, x)$ and $u_{22}(t_k, x)$ for $t_1 = 30$, $t_2 = 130$, $t_3 = 500$, and $a_1 = a_2 = 1$ in the case where reactants adsorb on both active and inactive in reaction surfaces. This figure shows that these functions change their concavity to convexity or vice versa as time grows: $u_{21}(30, x)$, $u_{21}(130)$, and $u_{22}(500, x)$ are concave, while $u_{21}(500, x)$, $u_{22}(30, x)$, and $u_{22}(130, x)$ are convex functions. Simulations reveal that the behavior of functions $u_{ji}(t_k, x)$, $k = 1, 2, 3$, $j = 1, 3, 4$, $i = 1, 2$, and the concavity and convexity of $u_{ji}(t_k, x)$ with all k, j, i in case where reactants adsorb on both active and inactive surfaces and only inactive surface, respectively, are similar to those given in Figs. 3 and 4.

5 Conclusions

In this paper, we proposed a phenomenological model described by a coupled system of PDEs for the carbon monoxide (CO) with nitrogen oxide (NO) reduction reaction proceeding over surfaces of supported catalysts. The model includes the adsorption and desorption of molecules of both reactants of the prescribed concentrations at the catalyst surface and the diffusion of adsorbed molecules. The surface diffusion is described by the jumping mechanism [7]. The adsorption, desorption, surface diffusion and reaction are allowed to proceed at a constant temperature.

By using the well-established finite-volume and finite-difference techniques the mathematical model is approximated by the discrete computational model. The proposed discrete scheme approximates the nonstandard conjugation conditions in a conservative way. The nonlinear space interaction of different components is resolved by rewriting the

model as a mass conservation equation with specific diffusion-advection fluxes. The upwind method is used to approximate the nonlinear advection terms. It is proved that the discrete solutions of specially selected subproblems inherit main properties of the solution of the full differential mathematical model.

The influence of the initial concentrations of both reactants and adsorption rate constants on the behavior of the catalyst surface turnover rates z_1, z_2, and z_3 were studied. Numerical analysis of the model with a broad range of parameter sets will be presented in a forthcoming paper, where an extended model will be given and studied. Results of numerical experiments show that the conversion rates z_1 and z_2 are decreasing functions of CO concentration for large t, but nonmonotonic ones for small t for NO concentration $a_1 = 1$. $z_1(t)$, as a function of NO concentration, has a maximum at $a_1 \approx 3$ when $a_2 = 1$. In case where both reactants adsorb only on the inactive in reaction support and $a_1 = a_2 = 1$, turn-over rates z_1, z_2, and z_3 are increasing functions of parameter $k_{11} = k_{21}$. In the same case, z_1, z_2, z_3 decrease as k_{21} grows; z_1, z_2 increase for small t and behave vice versa for large t, z_3 decreases for all t as k_{11} increase. The influence of the initial reactant concentrations on the behavior of concentrations $u_{ji}(t,x)$, $j,i = 1,2$, is also studied. Simulations reveal that $u_{ji}(t,x)$ is discontinuous at the catalyst-support interface and $u_{ji}(t,x)$ can change their concavity to convexity or vice versa as time grows.

Acknowledgment. We would like to thank the reviewers for their comments, which are very helpful and constructive.

References

1. A. Araújo, S. Barbeiro, P. Serranho, Stability of finite difference schemes for nonlinear complex reaction-diffusion processes, *IMA J. Numer. Anal.*, **35**:1381–1401, 2015.
2. B.K. Cho, Mechanistic importance of intermediate $N_2O + CO$ reaction in overall $NO + CO$ reaction system: I. Kinetic analysis, *J. Catal.*, **138**:255–265, 1992.
3. R. Čiegis, A. Bugajev, Numerical approximation of one model of the bacterial self-organization, *Nonlinear Anal. Model. Control*, **17**:253–270, 2012.
4. R. Čiegis, N. Tumanova, Stability analysis of implicit finite-difference schemes for parabolic problems on graphs, *Numer. Funct. Anal. Optim.*, **33**:1–20, 2012.
5. L. Cwiklik, B. Jagoda-Cwiklik, M. Frankowitz, Influence of the spacing between metal particles on the kinetics of reaction with spillover on the supported metal catalyst, *Appl. Surf. Sci.*, **252**:778–783, 2005.
6. A. Gerisch, J. Verwer, Operator splitting and approximate factorization for taxis-diffusion-reaction models, *Appl. Numer. Math.*, **42**:159–176, 2002.
7. A.N. Gorban, H.P. Sargsyan, H.A. Wahab, Quasichemical models of multi-component nonlinear diffusion, *Math. Model. Nat. Phenom.*, **6**:184–262, 2011.
8. P. Granger, L. Delannoy, J.J. Lecomte, C. Dathy, H. Praliaud, L. Leclercq, G. Leclercq, Kinetics of the $CO + NO$ reaction over bimetalic platinum-rhodium on alumina: Effect of ceria incorporation into noble metals, *J. Catal.*, **207**:202–212, 2002.

9. P. Granger, J.J. Lecomte, L. Leclercq, G. Leclercq, An attempt at modelling the activity of $\mathrm{Pt\text{-}Rh}/\mathrm{Al_2O_3}$ reaction, *Appl. Catal. A*, **208**:369–379, 2001.

10. W. Hundsdorfer, J.G. Verwer, *Numerical Solution of Time-Dependent Advection-Diffusion-Reaction Equations*, Springer Ser. Comput. Math., Vol. 33, Springer, Berlin, 2003.

11. T.G. Mattos, F.D.A. Aarão Reis, Effects of diffusion and particle size in a kinetic model of catalysed reactionst, *J. Catal.*, **263**:67–74, 2009.

12. A. Samarskii, *The Theory of Difference Schemes*, Marcel Dekker, New York, Basel, 2001.

13. I. Sergienko, V. Deineka, Models with conjugation conditions and high-accuracy methods of their discretization, *Cybern. Syst. Anal.*, **36**:83–101, 2000.

14. V. Skakauskas, P. Katauskis, Modelling dimer-dimer reactions on supported catalysts, *J. Math. Chem.*, **53**:604–617, 2015.

15. V. Skakauskas, P. Katauskis, Computational study of CO oxidation by $\mathrm{N_2O}$ reaction over supported catalysts, *J. Math. Chem.*, **54**:1306–1320, 2016.

16. V. Starikovičius, R. Čiegis, O. Iliev, A parallel solver for design of oil filters, *Math. Model. Anal.*, **16**:326–342, 2011.

17. V.P. Zhdanov, B. Kasemo, Mechanism and kinetics of the $\mathrm{NO}-\mathrm{CO}$ reaction on Rh, *Surf. Sci. Rep.*, **29**:31–90, 1997.